Original Article

Proposed clinical internal carotid artery classification system

ABSTRACT

Introduction: Numerical classification systems for the internal carotid artery (ICA) are available, but modifications have added confusion to the numerical systems. Furthermore, previous classifications may not be applicable uniformly to microsurgical and endoscopic procedures. The purpose of this study was to develop a clinically useful classification system.

Materials and Methods: We performed cadaver dissections of the ICA in 5 heads (10 sides) and evaluated 648 internal carotid arteries with computed tomography angiography. We identified specific anatomic landmarks to define the beginning and end of each ICA segment.

Results: The ICA was classified into eight segments based on the cadaver and imaging findings: (1) Cervical segment; (2) cochlear segment (ascending segment of the ICA in the temporal bone) (relation of the start of this segment to the base of the styloid process: Above, 425 sides [80%]; below, 2 sides [0.4%]; at same level, 107 sides [20%]; $P < 0.0001$) (relation of cochlea to ICA: Posterior, 501 sides [85%]; posteromedial, 84 sides [14%]; $P < 0.0001$); (3) petrous segment (horizontal segment of ICA in the temporal bone) starting at the crossing of the eustachian tube superolateral to the ICA turn in all 10 samples; (4) Gasserian-Clival segment (ascending segment of ICA in the cavernous sinus) starting at the petrolingual ligament (PLL) (relation to vidian canal on imaging: At same level, 360 sides [63%]; below, 154 sides [27%]; above, 53 sides [9%]; $P < 0.0001$); in this segment, the ICA projected medially toward the clivus in 275 sides (52%) or parallel to the clivus with no deviation in 256 sides (48%; $P < 0.0001$); (5) sellar segment (medial loop of ICA in the cavernous sinus) starting at the takeoff of the meningeal hypophyseal trunk (ICA was medial into the sella in 271 cases [46%], lateral without touching the sella in 127 cases [23%], and abutting the sella in 182 cases [31%]; $P < 0.0001$); (6) sphenoid segment (lateral loop of ICA within the cavernous sinus) starting at the crossing of the fourth cranial nerve on the lateral aspect of the cavernous ICA and located directly lateral to the sphenoid sinus; (7) ring segment (ICA between the 2 dural rings) starting at the crossing of the third cranial nerve on the lateral aspect of the ICA; (8) cisternal segment starting at the distal dural ring.

Conclusions: The classification may be applied uniformly to all skull base surgical approaches including lateral microsurgical and ventral endoscopic approaches, obviating the need for 2 separate classification systems. The classification allows extrapolation of relevant clinical information because each named segment may indicate potential surgical risk to specific structures.

Key words: Aneurysms; endoscopy; internal carotid artery skull base; tumors.

Saleem I Abdulrauf, Ahmed M Ashour, Eric Marvin, Jeroen Coppens, Brian Kang, Tze Yu Yeh Hsieh, Breno Nery, Juan R Penanes, Aysha K Alsahlawi, Shawn Moore, Hussam Abou Al-Shaar, Joanna Kemp, Kanika Chawla, Nanthiya Sujijantarat, Alaa Najeeb, Nadeem Parkar,[1] Vilaas Shetty,[1] Tina Vafaie, Jastin Antisdel,[2] Tony A Mikulec,[2] Randall Edgell,[3] Jonathan Lebovitz, Matt Pierson, Paulo Henrique Pires de Aguiar, Paula Buchanan,[4] Angela Di Cosola, George Stevens

Departments of Neurological Surgery, [1]Radiology, [3]Neurology, [2]Head and Neck Surgery and [4]Center for Outcomes Research, Saint Louis University, Saint Louis, Missouri, United States of America

Address for correspondence: Prof. Saleem I Abdulrauf, Department of Neurosurgery, Saint Louis University, 3635 Vista Avenue, 5-FDT, Saint Louis, MO, 63110 USA. E-mail: abdulrsi@slu.edu

How to cite this article: Abdulrauf SI, Ashour AM, Marvin E, Coppens J, Kang B, Hsieh TY, et al. Proposed clinical internal carotid artery classification system. J Craniovert Jun Spine 2016;7:161-70.

Introduction

Classification systems for the internal carotid artery (ICA) are numerically based, have been confused because of modifications, and do not apply uniformly to microsurgical and endoscopic approaches.

The purpose of the present study was to (1) develop a clinical-based classification system for the ICA; (2) identify anatomic landmarks that may define the beginning and the end of the segments of the ICA because of variation in length and angulation of the various ICA segments; (3) develop a system that may be applied uniformly to all surgical approaches to the base of the skull for lateral or ventral microsurgical or endoscopic procedures and avoid the need for 2 separate systems; and (4) design the classification system to enable extrapolation of relevant clinical information, so each named segment would highlight potential surgical risk to specific structures. The study was based on cadaver dissections and computed tomography angiography (CTA).

Materials and Methods

Cadaver study

We used 10 sides of 5 cadaver human heads that were fixed in formalin [Table 1]. The arterial system was injected with red latex through the cervical segment of the ICA, and the venous system was injected with blue latex through the internal jugular vein at the C6 vertebral level. The course of the ICA was delineated and examined with a microscope (OPMI PENTERO 900 microscope, Zeiss, Oberkochen, Germany). We evaluated the relation of the ICA to multiple fixed anatomic structures including the styloid process, cochlea, eustachian tube (ET), petrolingual ligament (PLL), abducens nerve, trigeminal nerve, gasserian ganglion, meningohypophyseal trunk (MHT), fourth cranial nerve, and third cranial nerve.

Table 1: Anatomic results in cadaver heads

Specimen number	Side	ICA wall diameter covered by ET laterally in mm	VI to PLL in mm	VI to MHT in mm
1	Right	9	6	4
2	Left	6	9	3
3	Left	4	9	4
4	Right	4	5	5
5	Right	4	7	3
6	Left	6	8	4
7	Right	9	6	3
8	Left	6	9	4
9	Right	7	6	5
10	Left	5	6	3

ICA - Internal carotid artery; PLL - Petrolingual ligament; ET - Eustachian tube; MHT - Meningohypophyseal trunk

Computed tomography angiography

The bony relations of the ICA to the base of the styloid process, cochlea, vidian canal, clivus, sella, and sphenoid sinus were studied with consecutive adult CTA images from the radiology database of our institution excluding those with documented pathology. The CTAs with thin, axial cuts were from 324 patients (648 sides). For each measurement, several studies were excluded because of limited image quality for the measurement. The following measurements were made.

- The relation of the base of the styloid process to the entrance of the ICA into the ICA canal was determined ($n = 534$), with the measurement determining whether the ICA canal was above, below, or at the level of the base of the styloid process
- A line bisecting the horizontal ICA in its petrous bony canal was extrapolated posteriorly, and its relation with the cochlea was evaluated. The position of the cochlea in relation to the ICA was recorded ($n = 586$), and we determined whether it was medial, at, or lateral to the bisecting line
- The bony distance between the anterior margin of the cochlea at its basal turn and the closest point of the ICA in the petrous canal was measured ($n = 586$)
- The relation of the beginning of the vidian canal was determined below, at the level of, or above the junction between the horizontal and ascending parts of the ICA in the cavernous sinus, close to the PLL ($n = 567$)
- The relation of the ascending segment of the ICA in the posterior part of the cavernous sinus to the clivus (ventral view) was determined as being medial, along the lateral edge of the clivus, or lateral to the clivus ($n = 531$)
- The relation of the medial loop of the ICA in the cavernous sinus to the lateral wall of the sella was determined ($n = 586$); the ICA was classified medially into the sella, abutted the sella, or remaining lateral without touching the sella
- The relation between the ICA and wall of the sphenoid sinus was examined for the presence of radiographic bony dehiscence, presence of the bony interval that separated the ICA from the sinus wall, and whether the ICA did not invade the wall and remained lateral.

Data analysis

All statistical analyses were performed using statistical software (QuickCalcs, GraphPad Software, San Diego, CA, USA). Chi-square goodness of fit was used to calculate P for equal distributions, assuming that the three categorical variables in the cochlea-ICA, ICA-clivus, ICA-dorsum sella, ICA-sphenoid, ICA-base of styloid, and ICA junction-vidian canal were equally distributed. Statistical significance was defined by $P \leq 0.05$.

Results

Cochlear segment: Ascending segment of the internal carotid artery in the temporal bone

The ascending segment of the ICA in the temporal bone started from the base of the styloid process and extended to the ET. In the 534 CTA studies, the beginning of the carotid canal was above the styloid process ($P < 0.0001$) [Table 2]. The cochlea was posterior to the horizontal course of the ICA where the ICA entered the petrous temporal bone, with an average bony interval between the cochlea and ICA in the axial plane of 2.22 mm (range, 0.2–11.8 mm; 95% confidence interval, 2.15–2.29 mm). The relation of the cochlea to the horizontal ICA was directly posterior [Figure 1] ($P < 0.0001$). In only 1 CTA (0.2%), the cochlea was posterolateral to the ICA [Figure 1]. After rising vertically through the petrous bone, the ICA turned anteriorly and medially. Based on these results, we named this ICA segment "cochlear segment" [Table 2].

Petrous segment: Horizontal segment of internal carotid artery in temporal bone

In all 10 cadaver sides, the horizontal segment of the ICA in the temporal bone started where the ET crossed the superolateral surface of the ICA, where the ICA course changed from vertical to horizontal at the genu. As the ICA entered the base of the skull through the carotid canal, it turned anteromedially at the genu to form the horizontal portion just anterior to the basal turn of the cochlea. The petrous segment ended where the beginning of the PLL crossed the ICA [Figure 2]. The superior surface of the genu was positioned directly medial to the bony part of the ET and tensor tympani muscle. The average thickness of the bony septum between the ET and the ICA was 6 mm (range, 4–9 mm) in all 10 cadaver sides, where the ET coursed anteriorly and inferiorly toward the nasopharynx [Figure 2]. Based on these findings, we adhered to the existing term, petrous, and further define it specifically to extent from the ET to the PLL [Tables 1 and 2].

Gasserian segment: Ascending segment of the internal carotid artery in the cavernous sinus

After coursing anteromedially through the petrous bone, the ICA ascended vertically toward the posterior part of the cavernous sinus. From the lateral (microsurgical) view, the ascending segment of the ICA in the posterior cavernous sinus started where the most proximal portion of the PLL crossed over the ICA (observed in all 10 cadaveric sides) and ended at the MHT. From the anterior (endoscopic) view, the junction between the petrous and this ascending segment of the ICA is marked by the vidian canal; in CTA images, this junction was at the level of the vidian canal in 360 sides (63%), below this level in 154 sides (27%), and above this level in 53 sides (9%) ($P < 0.0001$) [Figure 3]. From the ventral (endoscopic) view, this segment of ICA was projecting medially onto the clivus in 275 sides (52%), running along the lateral edge of the clivus in 256 sides (48%), and lateral to the clival edge without abutting the clivus in 0 sides ($P < 0.0001$) [Figure 3].

Table 2: Radiographic results

Relationship	Number of CTA (%)
Styloid base to ICA entrance into bony canal	
Above	425 (80)
At	107 (20)
Below	2 (0.4)
Total	534
Cochlea to ICA	
Lateral	1 (0.2)
At	501 (85)
Medial	84 (14)
Total	586
Vidian canal to the junction of petrous and Gasserian-clival ICA	
Above	53 (9)
At	360 (63)
Below	154 (27)
Total	567
ICA to sella	
Medial	271 (46)
Abutted	182 (31)
Lateral	133 (23)
Total	586
ICA - sphenoid	
Medial	183 (37)
Abutted	293 (59)
Lateral	20 (4)
Total	496

ICA - Internal carotid artery; CTA - Computed tomography angiography; ET - Eustachian tube
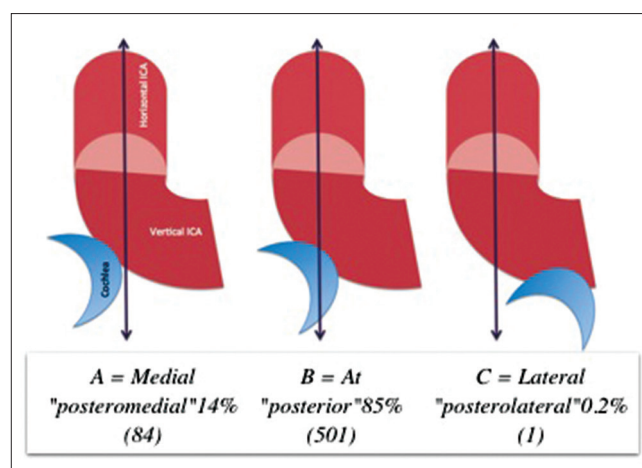

Figure 1: Relationship of the internal carotid artery to the Cochlea. Diagram depicting the right internal carotid artery viewed from above. The internal carotid artery was located (A) posteromedial, (B) directly posterior, or (C) posterolateral to the cochlea

The abducens nerve was observed crossing lateral to this segment of the ICA in all 10 cadaveric sides. The average length from the superior edge of the PLL to the 6th cranial nerve was 7.1 mm (range, 5–9 mm). The average interval between the MHT and the 6th cranial nerve was 3.8 mm (range, 3–5 mm) [Figure 4].

This segment of the ICA (from a lateral microsurgical perspective) was covered laterally by the trigeminal nerve ganglion (gasserian ganglion) in all 10 samples. This segment was also (from ventral endoscopic perspective) associated with the lateral border of the clivus in 100% of the CTA studies. Therefore, we named this segment "Gasserian-clival segment" [Tables 1 and 2].

Sellar segment: Medial loop of the internal carotid artery in the cavernous sinus

The medial loop of the ICA in the cavernous sinus started at the MHT in the posterior portion of the cavernous sinus
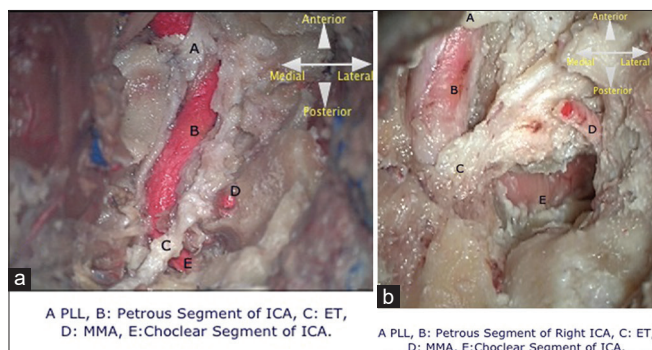

A PLL, B: Petrous Segment of ICA, C: ET, D: MMA, E:Choclear Segment of ICA.

A PLL, B: Petrous Segment of Right ICA, C: ET, D: MMA, E:Choclear Segment of ICA.

Figure 2: Cadaver dissection of the horizontal segment of the right internal carotid artery in the temporal bone. (a) The petrous segment ended where the beginning of the petrolingual ligament crossed the internal carotid artery. (b) The eustachian tube coursed anteriorly and inferiorly toward the nasopharynx. ET: Eustachian tube, ICA: Internal carotid artery, MMA: Middle meningeal artery; PLL: Petrolingual ligament
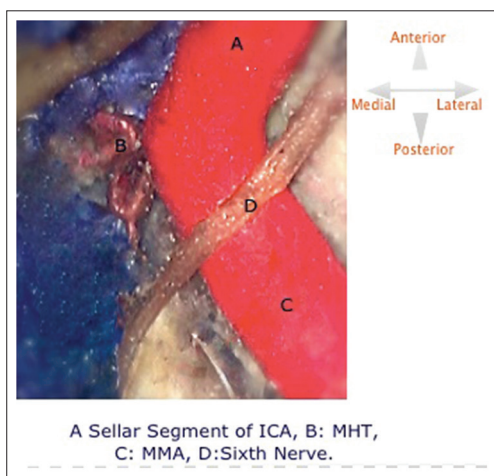

A Sellar Segment of ICA, B: MHT, C: MMA, D:Sixth Nerve.

Figure 4: Cadaver dissection (right lateral view) showing the internal carotid artery, abducens nerve, and meningohypophyseal trunk. MMA: Middle meningeal artery

and ended where the fourth nerve crossed the ICA laterally. This relation was observed in all 10 cadaver specimens. From a coronal cut of the ICA at the level of the MHT in the cadaveric specimens, the MHT was located at on the superior surface of the ICA in 9 sides, medial in 1 side, and lateral in 0 side [Figure 5]. In CTA axial sections, the ICA projected medially into the sella in 271 (46%), abutted the sella without projecting into it in 182 (31%), and was lateral without touching the sella in 127 (23%) ($P < 0.0001$) [Figure 6]. Therefore, we named this segment "sellar segment" [Tables 1 and 2].

Sphenoid segment: Lateral loop of the internal carotid artery within the cavernous sinus

The lateral loop of the ICA within the cavernous sinus started where the fourth nerve crossed the ICA in all 10 cadaveric sides (lateral microsurgical view) [Figures 7-10]. From a ventral view (endoscopic or microsurgical), this segment was coursing directly lateral to the sphenoid sinus in all 10 specimens. Bony dehiscence of the lateral sphenoid wall overlying this segment of the ICA was studied with CTA; complete bony dehiscence was observed in 183 sides (37%), the ICA abutted the sphenoid sinus wall without dehiscence in 293 sides (59%), and the
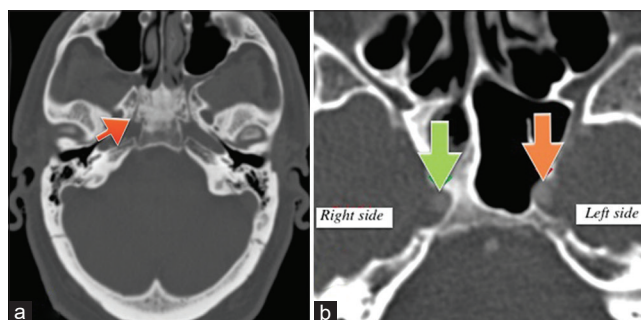

Figure 3: Ascending segment of the internal carotid artery in the cavernous sinus. (a) Axial computed tomography angiography image: The start of the vidian canal (posterior end of the canal) at the level of the junction of horizontal petrous and ascending cavernous internal carotid artery segments (arrow). (b) Axial computed tomography angiography image: The relation of the ascending segment of the internal carotid artery in the posterior cavernous sinus projecting medially into the sphenoid sinus shown on the left side (orange arrow) and running along the side of the clivus shown on the right side (green arrow)
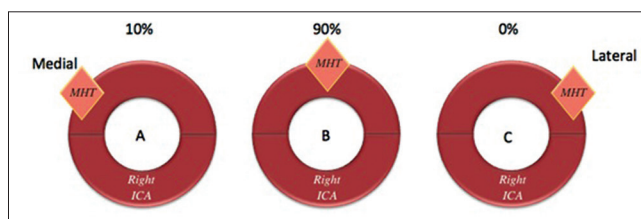

Figure 5: The site of the origin of the meningohypophyseal trunk based on the coronal depiction of the right internal carotid artery. (A) Meningohypophyseal trunk origin from the medial surface of the internal carotid artery. (B) Meningohypophyseal trunk origin from the superior surface of the internal carotid artery. (C) Meningohypophyseal trunk origin from the lateral surface of the internal carotid artery
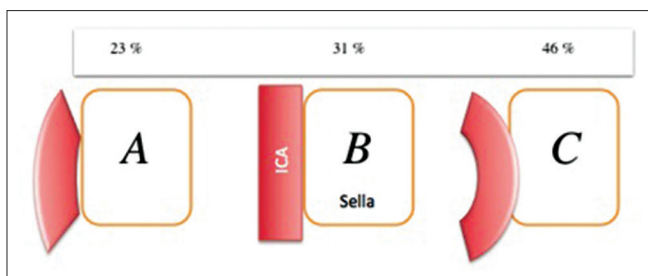
Figure 6: The internal carotid artery relation to the sella (diagrammatic axial depiction of the right internal carotid artery as seen from above). (A) Internal carotid artery not projecting into the sella wall. (B) Internal carotid artery abutting the sella wall. (C) Internal carotid artery projecting medially into the sella wall
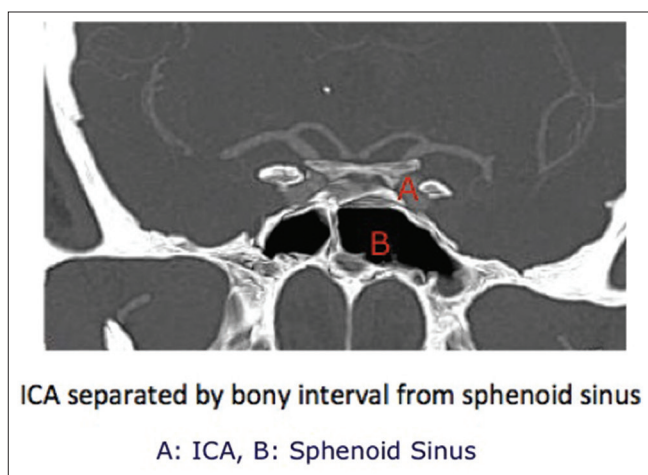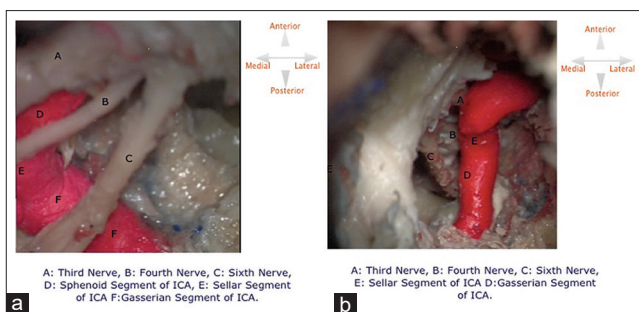

Figure 7: Lateral loop of the right internal carotid artery within the cavernous sinus (cadaveric dissection: Right lateral view (a) and anterior view (b))
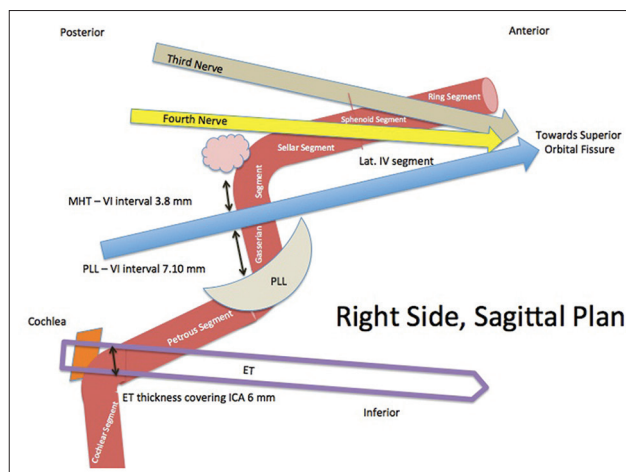

Figure 8: Coronal computed tomography angiography image depicting sphenoid segment

Figure 9: Diagrammatic illustration of the key anatomic junctions separating the proposed internal carotid artery segments

ICA did not touch the sphenoid sinus wall (no dehiscence) in 30 sides (4%) ($P < 0.0001$) [Figure 8]. Therefore, we named this segment "sphenoid segment" [Tables 1 and 2].

Ring segment: Internal carotid artery segment between the 2 rings

The ICA segment between the 2 rings started where the third nerve crossed the ICA and ended at the distal dural ring. The third nerve touched the ICA on its lateral side at the level of the proximal ring in all 10 cadaver specimens. The distal dural ring marked the termination of this ICA segment. Therefore, we named this segment "ring segment" [Figures 9 and 10, Tables 1 and 2].

Discussion

The present study provided a classification of the ICA that may define structures at risk during microsurgical or endoscopic approaches. The first classification system for the ICA was published by Fisher in 1938, which was based on angiographic data.[1] The Fisher's classification remained the standard

until 1981, when Gibo et al. introduced an anterograde classification of the ICA that divided the ICA into 4 segments, based on locations of aneurysms: The cervical ICA was the C1 segment; the intracranial ICA was subdivided into the petrous (C2) segment, cavernous (C3) segment that ended at the distal dural ring, and supraclinoid (C4) segment; and the C4 segment was divided into ophthalmic, communicating, and choroidal parts.[2] In 1987, Lasjaunias and Berenstein classified the ICA based on embryology.[3] In 1989, Dolenc added further details to the understanding of the cavernous segment of the ICA.[4] In 1990, Spetzler et al. provided anatomic and surgical details about the petrous segment of the ICA.[5] In 1996, Bouthillier et al. proposed a further modification of this system that is commonly used at present. This classification system divided the ICA into 7 segments, labeled C1 to C7 in an anterograde direction and was the first classification to include lacerum and clinoid segments.[6] In 2001, the initial experience with understanding the ICA from an endoscopic perspective was reported by Alfieri and Jho, who introduced the parasellar and paraclival terminology to segments of the ICA.[7] In 2005, Ziyal et al. proposed the removal of the lacerum segment because the ICA did not

pass through the foramen lacerum; they added a trigeminal segment and omitted the ophthalmic segment due to variability of its origin.[8] In 2008, Pfeiffer and Ridder described variations in the course of the cervical (parapharyngeal) ICA that may have clinical implications in otorhinolaryngology procedures.[9] Furthermore, in 2008, Osawa *et al.* provided the most detailed anatomic description of the petrous carotid in the literature.[10] In 2012, Fortes *et al.* provided the results of anatomic dissections that exposed the ICA through an endoscopic transpterygoid approach.[11] In 2013, Wang *et al.* used CTA and subclassified the cavernous ICA for endoscopic approaches.[12] In 2014, Labib *et al.* provided a detailed scheme based on cadaver dissections for classification of the ICA for ventral endoscopic approaches.[13] In 2014, DePowell *et al.* performed ventral endoscopic dissections in 5 cadavers and proposed that the classification of Bouthillier *et al.* from 1996 could be applied for ventral endoscopic approaches.[6,14] In 2014, Shapiro *et al.* proposed a classification based on branching points of the ICA for endovascular procedures,[15] and Cebula *et al.* identified 4 anatomic patterns of the carotid siphon in relation to the pituitary gland using cadaveric specimens.[16] The seven decades of work by researchers in neurosurgery, otorhinolaryngology, radiology, and neurology who studied the ICA may be summarized into three categories: (1) Angiographic classification systems, (2) cadaver neuroanatomic descriptions, and (3) ventral endoscopic observations of the ICA. The endoscopic understanding of the ICA is important because of the increased use of endoscopic approaches to the base of the skull that may cause ICA injury or pseudoaneurysm after ventral endoscopic approaches.[2,5,6,9,10,13,17-29] The numerical classification systems may be confusing because of changes in the numerical systems based on updated findings. In proposing the present classification system, we added information about associated structures to each segment, based on detailed statistical analysis, which may be valuable in alerting the surgeon about structures at risk, depending on the surgical zone, during lateral microsurgical or ventral endoscopic procedures [Table 3]. In addition, we provided specific landmarks to define the beginning and end of each segment [Figure 11].

We review our findings and classification system.

Cervical segment

We retained the historical terminology of the extracranial cervical segment of the ICA as defined previously. We did not study this segment anatomically or radiographically because the naming and anatomy of this segment were well established in the literature. In our classification system, we defined the
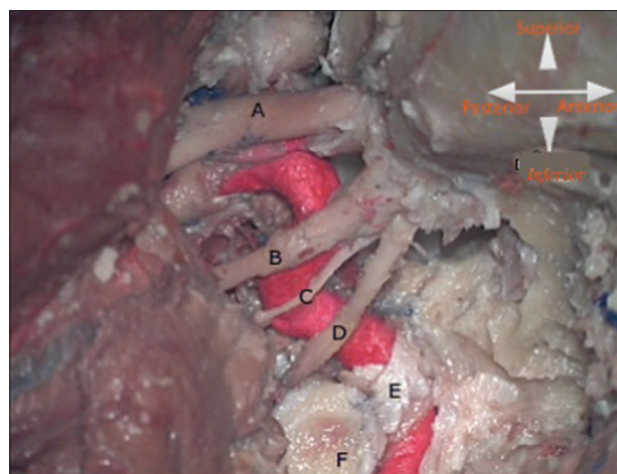

Figure 10: Cadaveric specimen demonstrating petrous, Gasserian-Clival, sellar, sphenoidal, and ring Segments (right lateral view). A: Second nerve, B: Third nerve, C: Fourth nerve, D: Sixth nerve, E: PLL, Cochlea, Yellow: Petrous red: Gasserian, Orange: Sellar, Green: Sphenoid, Blue: Ringt, Dark Green: Subarachnoid segments of ICA
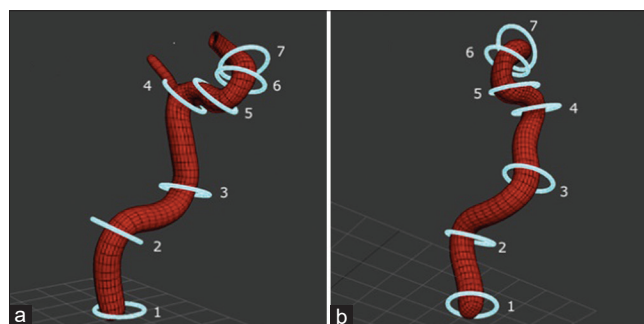

Figure 11: Three-dimensional reconstruction of the internal carotid artery based on data points collected. Image depicting the 7 transition anatomic landmarks (blue rings depicting each specific anatomic point). (a) Lateral view of the right internal carotid artery. (b) Anterior view of the right internal carotid artery. (1) Base of the styloid mastoid foramen (2) ET (3) PLL (4) MHT (5) 4th (6) 3rd CN (7) Distal ring
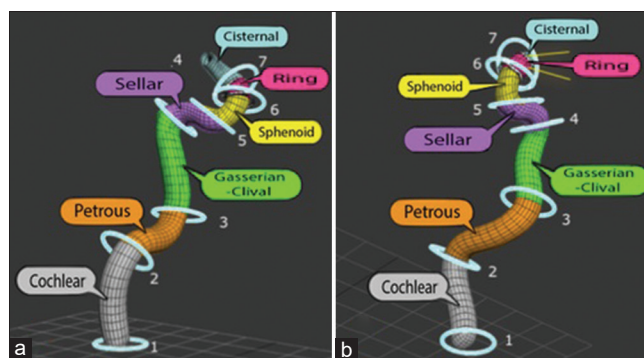

Figure 12: Three-dimensional reconstruction of the internal carotid artery based on data points collected. Image depicting the 7 transition anatomic landmarks (blue rings). Color- coded proposed internal carotid artery segments. (a) Lateral view of the right ICA. (b) Anterior view f the right ICA. The blue rings are delineating the transitional points of each segment of the ICA based on the findings of the study. (1) Base of the styloid mastoid foramen (2) ET (3) PLL (4) MHT (5) 4th (6) 3rd CN (7) Distal ring

end of the cervical and beginning of the cochlear segment at the base of the styloid process [Table 2 and Figure 12].

Cochlear segment

We defined the cochlear segment from the base of the styloid process to the level of the ET where the ET crosses the ICA laterally [Figure 12]. The bone between the petrous carotid canal and cochlea in the axial plane had average thickness 2.2 mm. The cochlear segment is not encountered in most approaches to the base of the skull, but it is exposed in the approach to total petrosectomy, during which it is necessary to drill the cochlea to access this segment. Our findings related the aforementioned surgical trajectory to the naming of this segment.

Petrous segment

The petrous segment was defined as starting where the ET crosses the ICA laterally and ending at the beginning of the PLL (lateral view) and proximal portion of the vidian canal (ventral endoscopic view) [Tables 1 and 2, Figures 12 and 13]. From the lateral microsurgical perspective, this segment of the ICA can be exposed for proximal control during surgery for aneurysms or skull base tumors. This segment also may be at risk of injury during the drilling of the petrous apex [Table 3]. From the ventral endoscopic perspective, this segment may be at risk during dissection or drilling in a plane lateral to the vidian canal [Figure 13]. The vidian canal previously was defined as a landmark for the petrous ICA by Kassam *et al*.,[26,30] and our work further confirmed the importance of this landmark.

Gasserian-clival segment

The gasserian segment was defined as starting at the PLL (lateral view) and proximal vidian canal (ventral view) and

Figure 13: Three-dimensional reconstruction of the internal carotid artery based on data points collected. The vidian canal and its three-dimensional relation to the junction of the petrous to the Gasserian-Clival internal carotid artery segments (a). The Vidian canal and the eustachian tube and their relationship to the cochlear, petrous, and Gasserian-Clival segments (b). (a) Anterior view of the both ICA. (b) Coronal view of the both ICA. (1) ET (2) Vidan Canal, (A) Cohlear, (B) petrous, (C) Gasserian – Clival (D) Sellar (E) Sphenoid (F) Ring (G) Cisternal segments of the ICA

ending at the MHT [Table 1 and Figure 12]. Although the PLL was used as a landmark in previous classifications, it may have limited clinical application because it may not be demonstrated on radiography. The proximal vidian canal is a better landmark for the start of this segment. From the anterior or endoscopic approach, the proximal end of the vidian canal is located at the junction of the petrous and gasserian segments. There are variations in the course of the vidian canal in relation to the sphenoid sinus.[11,30-33] From the microsurgical prospective, this segment is important during surgery of Meckel's cave, and our results showed that the sleeve of the gasserian ganglia may cover the lateral surface of this ICA segment. Therefore, from a lateral microsurgical perspective, the surgery of Meckel's cave may be associated with injury of the gasserian segment of the ICA [Table 3]. From the ventral endoscopic perspective, our results showed that this segment is in the superior plane of the proximal vidian canal [Table 2, Figures 12 and 13].

Exposure of the gasserian segment of the ICA is rarely required for microsurgical lateral approaches because it is in the posterior portion of the cavernous sinus. The recognition of this segment is however clinically important when operating on tumors involving Meckel's cave such as schwannoma or meningioma as this segment of the ICA is directly medial in these microsurgical procedures. For ventral endoscopic approaches involving the clivus, our study showed that there is an important surgically relevant relation between this segment of the ICA and the lateral border of the upper clivus. We specially noted that in approximately 50% of the CTAs, the ICA actually projected medially toward the clivus from its lateral border zone, and thus a potential risk of ICA injury during these endoscopic approaches. In addition, this relation of the ICA to the clivus is pertinent only at and above the vidian canal because the Gasserian-clival segment did not extend below the
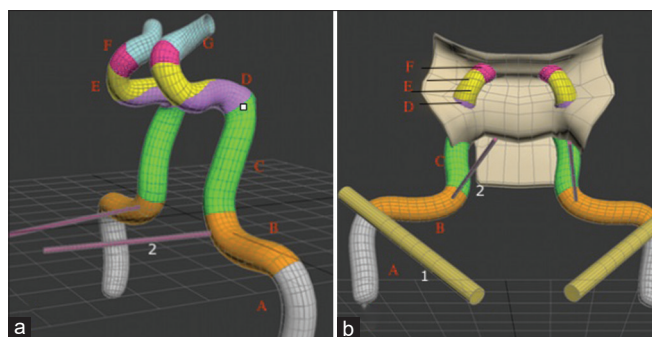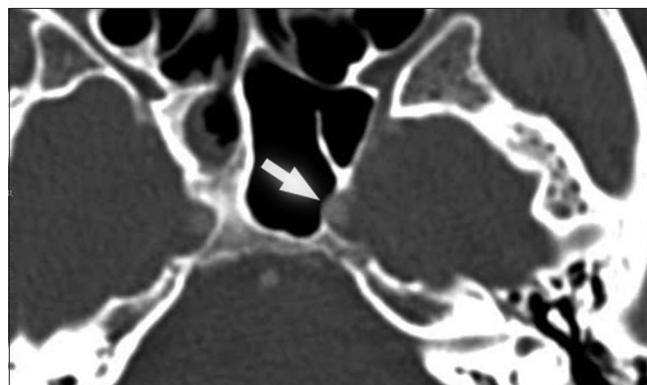

Figure 14: Axial computed tomography angiography image demonstrating bony dehiscence at the Gasserian-Clival segment of the internal carotid artery (white arrow)

vidian canal on the clivus in any of the scans. Therefore, to obtain lateral access along the clivus in ventral transclival approaches, we recommend identifying the vidian canal and obtaining access laterally on the clivus below the level of the vidian canal [Figure 14].

Sellar segment

The sellar segment started at the origin of the MHT and ended at the level where the fourth cranial nerve crossed the ICA laterally [Table 1 and Figure 12]. The MHT and artery of Bernasconi and Cassinari, which is a tentorial branch of the MHT, are feeders for neoplasms and vascular malformations of the tentorium cerebelli.[34] Petroclival tumors may be devascularized during extradural dissection and the cutting of the tentorium with ligation of the MHT.[22,34,35] The MHT may be exposed through the infratrochlear triangle because it is located within the posterior compartment of the cavernous sinus.[36] The clinical importance of this segment is the potential risk of injury to the ICA during transsphenoidal procedures. Based on our findings, the sellar segment is the ICA segment that is closest to the sella and pituitary gland [Table 3]; Cebula *et al.* previously showed that in 80% specimens, the ICA (sellar segment in our classification system) was in direct contact with the pituitary gland [Figure 15].[16]

Sphenoid segment

The sphenoid segment started where the fourth nerve crossed the ICA laterally and ended where the third cranial nerve crossed the ICA laterally. This segment is important in endoscopic approaches to the sphenoid sinus and sella. The sphenoid segment lies superior and lateral in the sphenoid sinus and forms the lower margin of the lateral optical carotid recess. The risk of ICA injury inside the sphenoid sinus may be associated with dehiscence of bone in this segment (as

demonstrated in our study of complete dehiscence in 37% of the CTAs) or drilling lateral to the optical carotid recess without full recognition of the course of the sphenoid segment [Figure 16].

Ring segment

The ring segment started where the third nerve crossed the ICA laterally (proximal ring) and ended at the distal dural ring. This segment is important during anterior clinoid drilling for aneurysms involving the ophthalmic segment of the ICA. The start of the ring segment demarcates the point of the end of the cavernous sinus.

Cisternal segment

The cisternal segment started from the distal dural ring and ended at the bifurcation of the ICA. Classification of this segment has been provided in detail previously[2,26,32,35,37-44] [Table 3].

Table 3: Classification system impact of identifying structures at risk

Surgical approach	Structure at risk
Total petrosectomy	Cochlear ICA segment
Extradural middle fossa dissection/drilling lateral to the ICA	ET
Drilling the petrous apex	Petrous ICA segment
Endoscopic dissection/drilling at the proximal vidian canal	Petrous-gasserian ICA junction
Endoscopic drilling lateral to the vidian canal	Petrous ICA segment
Endoscopic drilling superior to the vidian canal	Gasserian ICA segment
Anterior microsurgical or endoscopic drilling/dissection at lateral edge of clivus	Gasserian ICA segment
Microsurgical dissection In Meckel's cave	Gasserian ICA segment
Endoscopic or microsurgical dissection in the sella	Sellar ICA segment
Endoscopic or microsurgical dissection/drilling in the sphenoid sinus	Sphenoid ICA segment
Drilling of anterior clinoid and opening of proximal dural ring	Third cranial nerve

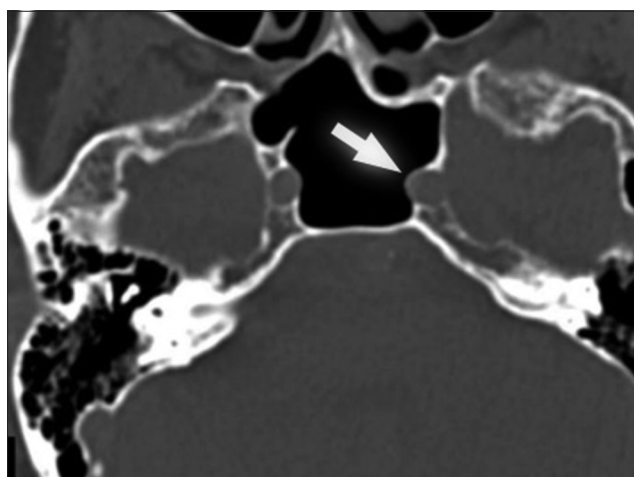ICA - Internal carotid artery; ET - Eustachian tube

Figure 15: Axial computed tomography angiography image demonstrating bony dehiscence at the sellar segment of the internal carotid artery (white arrow)
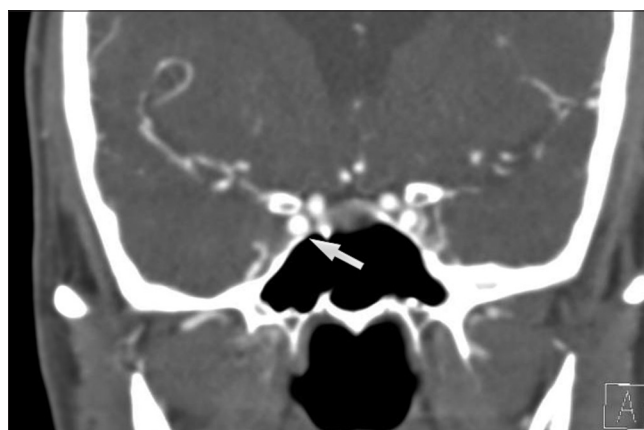

Figure 16: Coronal computed tomography angiography image demonstrating bony dehiscence at the sphenoid segment of the internal carotid artery (white arrow)
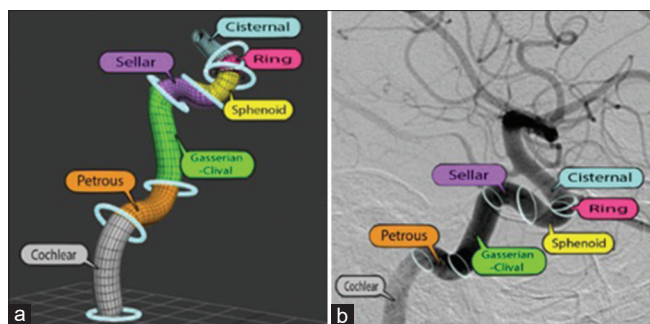
Figure 17: Summary of proposed internal carotid artery segments. (a) Three-dimensional reconstruction of the internal carotid artery based on data points collected. Color-coded system for each segment. Blue rings depicting the 7 anatomic landmarks marking the transition points. (b) Digital subtraction angiography with extrapolated proposed internal carotid artery classification

Conclusions

We classified the ICA into cervical, cochlear, petrous, Gasserian-clival, sellar, sphenoid, ring, and cisternal segments. Each segment started with a defined anatomic landmark. This system is simpler than previous systems, is reproducible, and helps define structures at risk during microsurgical and endoscopic approaches to the base of the skull. The classification also may unify ICA terminology between neurosurgery, head and neck surgery, neurology, and radiology. We propose that this system may be extrapolated to describe digital subtraction angiography of the ICA [Figure 17].

Conflicts of interest
There are no conflicts of interest.

References

1. Fischer E. The positional deviations of the anterior cerebral artery in Gefassbild. Zentralbl Neurochir 1938;3:300-13.
2. Gibo H, Lenkey C, Rhoton AL Jr. Microsurgical anatomy of the supraclinoid portion of the internal carotid artery. J Neurosurg 1981;55:560-74.
3. Lasjaunias P, Berenstein A. Arterial anatomy: Introduction. In: Surgical Neuroangiography. Springer-Verlag Berlin Heidelberg: Springer Science + Business Media; 1987. p. 1-32.
4. Dolenc VV. Intracavernous (saccular, fusiform) aneurysms of the internal carotid artery. In: Anatomy and Surgery of the Cavernous Sinus. Springer-Verlag Berlin Heidelberg: Springer Science+Business Media; 1989. p. 221-67.
5. Spetzler RF, Fukushima T, Martin N, Zabramski JM. Petrous carotid-to-intradural carotid saphenous vein graft for intracavernous giant aneurysm, tumor, and occlusive cerebrovascular disease. J Neurosurg 1990;73:496-501.
6. Bouthillier A, van Loveren HR, Keller JT. Segments of the internal carotid artery: A new classification. Neurosurgery 1996;38:425-32.
7. Alfieri A, Jho HD. Endoscopic endonasal cavernous sinus surgery: An anatomic study. Neurosurgery 2001;48:827-36.
8. Ziyal IM, Ozgen T, Sekhar LN, Ozcan OE, Cekirge S. Proposed classification of segments of the internal carotid artery: Anatomical study with angiographical interpretation. Neurol Med Chir (Tokyo) 2005;45:184-90.
9. Pfeiffer J, Ridder GJ. A clinical classification system for aberrant internal carotid arteries. Laryngoscope 2008;118:1931-6.
10. Osawa S, Rhoton AL Jr., Tanriover N, Shimizu S, Fujii K. Microsurgical anatomy and surgical exposure of the petrous segment of the internal carotid artery. Neurosurgery 2008;63 4 Suppl 2:210-38.
11. Fortes FS, Pinheiro-Neto CD, Carrau RL, Brito RV, Prevedello DM, Sennes LU. Endonasal endoscopic exposure of the internal carotid artery: An anatomical study. Laryngoscope 2012;122:445-51.
12. Wang C, Xie J, Cui D, Cheng Y, Zhang S. A new classification of cavernous segment of the internal carotid artery. J Craniofac Surg 2013;24:1418-22.
13. Labib MA, Prevedello DM, Carrau R, Kerr EE, Naudy C, Abou Al-Shaar H, *et al*. A road map to the internal carotid artery in expanded endoscopic endonasal approaches to the ventral cranial base. Neurosurgery 2014;10 Suppl 3:448-71.
14. DePowell JJ, Froelich SC, Zimmer LA, Leach JL, Karkas A, Theodosopoulos PV, *et al*. Segments of the internal carotid artery during endoscopic transnasal and open cranial approaches: Can a uniform nomenclature apply to both? World Neurosurg 2014;82 6 Suppl: S66-71.
15. Shapiro M, Becske T, Riina HA, Raz E, Zumofen D, Jafar JJ, *et al*. Toward an endovascular internal carotid artery classification system. AJNR Am J Neuroradiol 2014;35:230-6.
16. Cebula H, Kurbanov A, Zimmer LA, Poczos P, Leach JL, De Battista JC, *et al*. Endoscopic, endonasal variability in the anatomy of the internal carotid artery. World Neurosurg 2014;82:e759-64.
17. Takahashi M, Killeffer F, Wilson G. Iatrogenic carotid cavernous fistula. Case report. J Neurosurg 1969;30:498-500.
18. Lister JR, Sypert GW. Traumatic false aneurysm and carotid-cavernous fistula: A complication of sphenoidotomy. Neurosurgery 1979;5:473-5.
19. Matsuno A, Yoshida S, Basugi N, Itoh S, Tanaka J. Severe subarachnoid hemorrhage during transsphenoidal surgery for pituitary adenoma. Surg Neurol Int 1993;39:276-8.
20. Ciric I, Ragin A, Baumgartner C, Pierce D. Complications of transsphenoidal surgery: Results of a national survey, review of the literature, and personal experience. Neurosurgery 1997;40:225-36.
21. Cappabianca P, Briganti F, Cavallo LM, de Divitiis E. Pseudoaneurysm of the intracavernous carotid artery following endoscopic endonasal transsphenoidal surgery, treated by endovascular approach. Acta Neurochir (Wien) 2001;143:95-6.
22. Cho CW, Al-Mefty O. Combined petrosal approach to petroclival meningiomas. Neurosurgery 2002;51:708-16.
23. Kadyrov NA, Friedman JA, Nichols DA, Cohen-Gadol AA, Link MJ, Piepgras DG. Endovascular treatment of an internal carotid artery pseudoaneurysm following transsphenoidal surgery. Case report. J Neurosurg 2002;96:624-7.
24. Kizilkilic O, Albayram S, Adaletli I, Kantarci F, Uzma O, Islak C, *et al*. Endovascular treatment of ruptured intracranial aneurysms during pregnancy: Report of three cases. Arch Gynecol Obstet 2003;268:325-8.
25. Dusick JR, Esposito F, Malkasian D, Kelly DF. Avoidance of carotid artery injuries in transsphenoidal surgery with the Doppler probe and micro-hook blades. Neurosurgery 2007;60 4 Suppl 2:322-8.

26. Kassam AB, Engh JA, Mintz AH, Prevedello DM. Completely endoscopic resection of intraparenchymal brain tumors. J Neurosurg 2009;110:116-23.

27. Raymond J, Hardy J, Czepko R, Roy D. Arterial injuries in transsphenoidal surgery for pituitary adenoma; the role of angiography and endovascular treatment. AJNR Am J Neuroradiol 1997;18:655-65.

28. Al-Mefty O. Operative atlas of meningioma. In: Al-Mefty O, editor. Operative Atlas of Meningioma. New York: Lippincott-Raven; 1998. p. 209-348.

29. de Souza JM, Domingues FS, Espinosa G, Gadelha M. Cavernous carotid artery pseudo-aneurysm treated by stenting in acromegalic patient. Arq Neuropsiquiatr 2003;61:459-62.

30. Kassam AB, Vescan AD, Carrau RL, Prevedello DM, Gardner P, Mintz AH, *et al.* Expanded endonasal approach: Vidian canal as a landmark to the petrous internal carotid artery. J Neurosurg 2008;108:177-83.

31. Reddy K, Lesiuk H, West M, Fewer D. False aneurysm of the cavernous carotid artery: A complication of transsphenoidal surgery. Surg Neurol 1990;33:142-5.

32. Cavallo LM, Messina A, Gardner P, Esposito F, Kassam AB, Cappabianca P, *et al.* Extended endoscopic endonasal approach to the pterygopalatine fossa: Anatomical study and clinical considerations. Neurosurg Focus 2005;19:E5.

33. Prevedello DM, Ditzel Filho LF, Solari D, Carrau RL, Kassam AB. Expanded endonasal approaches to middle cranial fossa and posterior fossa tumors. Neurosurg Clin N Am 2010;21:621-35, vi.

34. Abdulrauf SI, Al-Mefty O. The petrosal approach. Neurosurgery 1999;2:58-61.

35. Hakuba A, Nishimura S, Tanaka K, Kishi H, Nakamura T. Clivus meningioma: Six cases of total removal. Neurol Med Chir (Tokyo) 1977;17(1 Pt 1):63-77.

36. Rhoton AL Jr. The supratentorial arteries. Neurosurgery 2002;51 (4 Suppl):S53-120.

37. Perlmutter D, Rhoton AL Jr. Microsurgical anatomy of the anterior cerebral-anterior communicating-recurrent artery complex. J Neurosurg 1976;45:259-72.

38. Gibo H, Carver CC, Rhoton AL Jr., Lenkey C, Mitchell RJ. Microsurgical anatomy of the middle cerebral artery. J Neurosurg 1981;54:151-69.

39. Pedroza A, Dujovny M, Artero JC, Umansky F, Berman SK, Diaz FG, *et al.* Microanatomy of the posterior communicating artery. Neurosurgery 1987;20:228-35.

40. Ferreira A, Braga FM. Microsurgical anatomy of the anterior choroidal artery. Arq Neuropsiquiatr 1990;48:448-53.

41. Marinkovic S, Gibo H. The neurovascular relationships and the blood supply of the oculomotor nerve: The microsurgical anatomy of its cisternal segment. Surg Neurol 1994;42:505-16.

42. Laws ER Jr. Vascular complications of transsphenoidal surgery. Pituitary 1999;2:163-70.

43. Falcon RT, Rivera-Serrano CM, Miranda JF, Prevedello DM, Snyderman CH, Kassam AB, *et al.* Endoscopic endonasal dissection of the infratemporal fossa: Anatomic relationships and importance of eustachian tube in the endoscopic skull base surgery. Laryngoscope 2011;121:31-41.

44. Rhoton AL Jr., Fujii K, Fradd B. Microsurgical anatomy of the anterior choroidal artery. Surg Neurol Int 1979;12:171-87.